

Development of Pyrazolo[3,4-*d*]pyrimidine Kinase Inhibitors as Potential Clinical Candidates for Glioblastoma Multiforme

Chiara Greco,[†] Vincenzo Taresco,[‡] Amanda K. Pearce,[§] Catherine E. Vasey,[⊥] Stuart Smith,[¶] Ruman Rahman,[¶] Cameron Alexander,[⊥] Robert J. Cavanagh,^{⊥,*} Francesca Musumeci,^{†,*} Silvia Schenone[†]

[†] Department of Pharmacy, University of Genoa, Viale Benedetto XV 3, 16132 Genoa, Italy

[‡] School of Chemistry, University of Nottingham, University Park, Nottingham NG7 2RD, UK

[§] School of Chemistry, University of Birmingham, Edgbaston, Birmingham B15 2TT, U.K

[⊥] School of Pharmacy, University of Nottingham, University Park, Nottingham NG7 2RD, U.K.

[¶] Children's Brain Tumour Research Centre, School of Medicine, University of Nottingham, Nottingham NG7 2UH, UK

Table of contents

Chemicals, page S1

Printing, page S1

Dynamic Light Scattering (DLS), page S2

UV screening, page S2

ΔA% determination, page S4

Cell lines, page S4

Determination of Combination Index (CI) values, page S7

References, page S7

Chemicals

Polyvinylpyrrolidone-vinyl acetate copolymer (PVPVA), Tween 80, Pluronic F-68 and dimethyl sulfoxide (DMSO) were purchased from SIGMA Aldrich and the latter used as a common solvent to dissolve all the printable materials. Synthesis of pyrazolo[3,4-*d*]pyrimidines kinase inhibitors were performed by Prof. Schenone's group at the University of Genoa.^{1,2,3}

Printing

Prior to dispensing the drug solution into a 96-well plate, the target had to be programmatically defined. The probe substrate consists of the well plate, drug solutions were dispensed via a piezoelectric inkjet printer (Sciflexarray S5, Scienion) using a 90 μm orifice nozzle. The droplet size was controlled by the values of the voltage and electrical pulse. A fixed amount of drug (20 μg) was dispensed for each well, by adjusting the number of drops. The number of drops per spot were selected in such way that the volume aspired delivered by the nozzle (max 10 μL) at the

beginning of a run was sufficient to print the whole print pattern. In a routine experiment DMSO solution (10 mg/mL) droplets with nominal volumes ranging from 250-280 pL, were dispensed at a 300 Hz jetting frequency by adjusting the voltage and pulse between 98-105 Volt (Voltage) and 45-55 μ s (Pulse) respectively. The nozzle was washed with DMF, in between each printing cycle, as part of the automated printing-washing loop. DMSO was chosen due to both its high evaporation point that avoids nozzle blockage and its ability to dissolve all the selected drugs. SI306 and polymer solutions were prepared by dissolving the desired amount of compound in DMSO and, separately, the polymers in deionized (DI) water, in order to reach a final concentration of 5 μ g/mL and 45 μ g/mL, respectively.

Dynamic Light Scattering (DLS)

Dynamic Light Scattering (DLS) measurements were conducted in triplicate using a Malvern Zetasizer Nano ZS at 25°C (scattering angle 173°, laser of 633 nm) or a Viscotek 802 DLS with a laser wavelength of 830 nm at 20 °C. Formulations were prepared as above at 5 μ g/mL (with respect to drug) in PBS. Data was analyzed using OmniSIZE software. A minimum of 10 measurements were collected per sample.

As can be observed from Figure 6 of the manuscript, all the formulations produced well-defined nanoaggregates, characterised by a single monomodal and monodispersed population with sizes ranging from 180 to 200 nm. The absence of a second peak or species related to aggregation confirmed the quality of the nanoformulation obtained due to the interactions between the small molecules and the different polymers. The amphiphilic nature of the macromolecules facilitated the interactions with the hydrophobic active compounds leading to an improvement of the self-assembly properties.

UV screening

Different commercial polymers (PEG8000, PEG20000, Pluronic F-68, Tween 80, PVPVA) were combined with SI306 (at a “drug”/polymer ratio of 10/90% w/w) and the apparent-solubility (Δ A%) value of each formulation was calculated in order to identify the polymers able to solubilise our lead compound. UV-vis spectra of SI306, commercial polymers and SI306-polymer formulations are reported in Figures 1SI and 2SI. Samples were diluted until the final concentration of 100 μ g/mL and 900 μ g/mL for SI306 and the polymers, respectively.

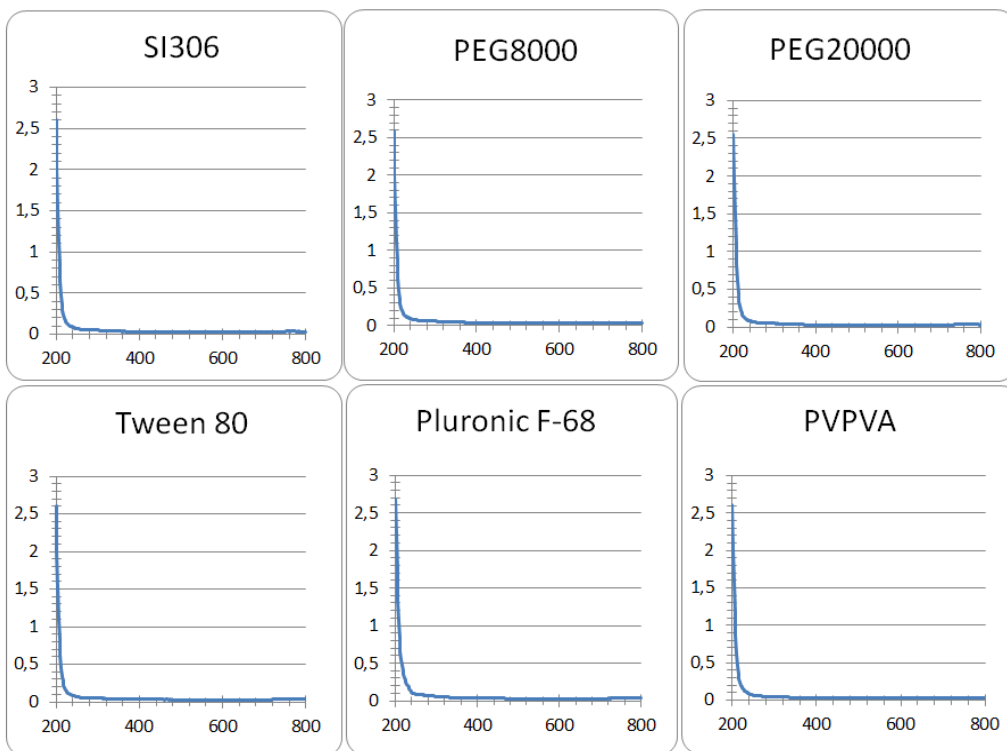


Figure 1SI. UV-vis spectra of SI306 (concentration 100 $\mu\text{g/mL}$) and selected commercial polymers (concentration 900 $\mu\text{g/mL}$) in PBS. We already demonstrated that solutions of in-house pyrazolo[3,4-*d*]pyrimidines in DMSO absorb in the UV region.⁴

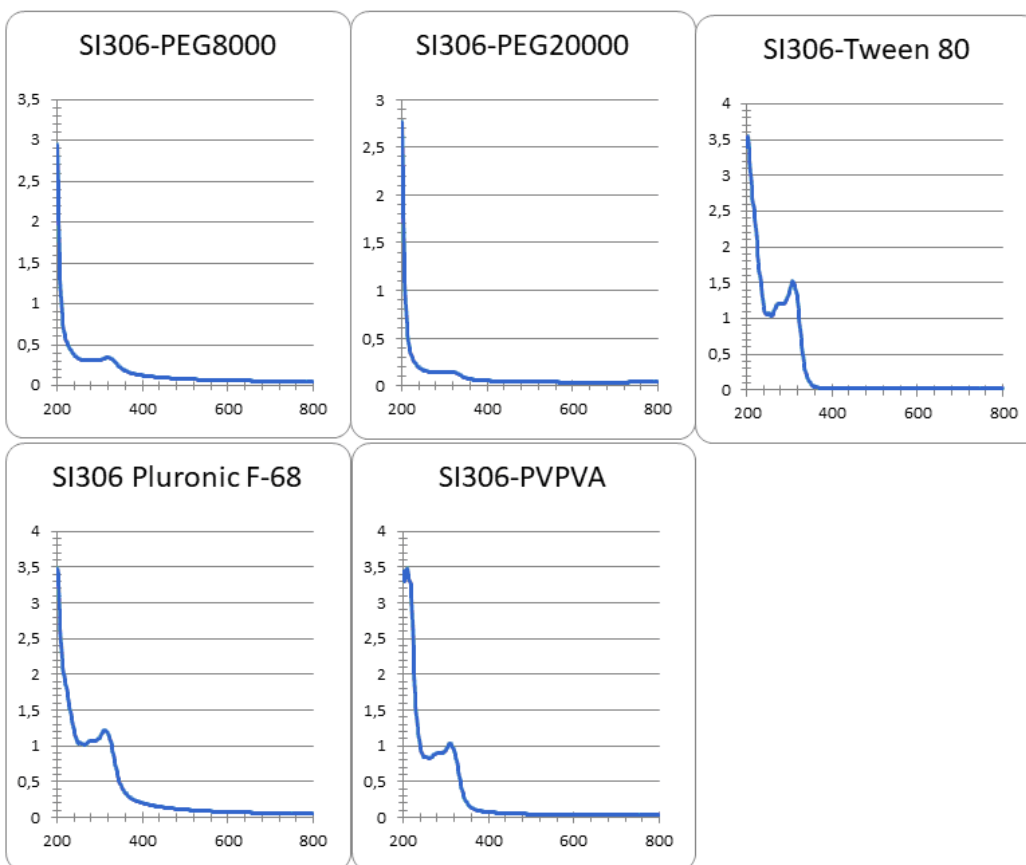


Figure 2SI. UV-vis spectra of SI306-polymer formulations in PBS (100 $\mu\text{g/mL}$ of SI306 and 900 $\mu\text{g/mL}$ of polymer).

ΔA% determination

ΔA% was calculated according the following equation:⁴

$$\Delta A\% = \frac{A - A_0}{A_0} \cdot 100$$

Where:

A₀ is the absorbance of the polymer solutions in water (used as blank),

A is the absorbance of the aqueous solutions of drug/polymer blends.

No signal was observed from the presence of water-insoluble SI306 (Figure 1SI).

In Table 1SI the ΔA% is reported for every SI306-polymer formulation.

Table 1SI. ΔA% of SI306 and polymers. Absorbance has been measured at λ = 308 nm

	PEG8000	PEG20000	Tween80	Pluronic F68	PVPVA
ΔA%	584.5179	555.3168	4251.295	2857.245	2312.342

Cell lines

GIN-8 (Glioma Invasive margin cells) isolated from medial front invasive margin (54F Wild type IDH (primary GBM), intact ATRX, 0% MGMT promoter methylation, 90% resection plus Gliadel wafers; Treatment 60Gy radiotherapy, concurrent and adjuvant temozolomide; patient died 5months after surgery), GIN-28 isolated from 5-ALA fluorescense invasive margin (71M Wild type IDH (primary GBM), intact ATRX, 0% MGMT promoter methylation 99% resection; no adjuvant therapy (patient choice); died 3 months after surgery) and GCE-28 (Glioma Contrast Enhanced core cells) isolated from central enhanced core region (same patient as GIN28) by Dr. Smith Dr. Rahman, and were used at passages of 15-30. Single tandem repeat (STR) genotyping is detailed in the **Figure 3SI**. The samples were paraffin-embedded and sectioned by the Queen's Medical Centre Histopathology Department. Cell lines were cultured in Dulbecco's Modified Eagle Medium (DMEM; Sigma-Aldrich) supplemented with 10% HyClone™ Bovine Growth Serum (BGS; GE Healthcare), 1g/L Glucose and 2 mM L-glutamine (Sigma-Aldrich) at 37°C with 5% CO₂.

DNA-System	DNA-criteria GIN-8 p11 CL181019_012	DNA-criteria GIN-8 p33 CL181019_013	DNA-criteria T8.3 CL181019_014	DNA-criteria GIN-28 p11 CL181019_021	DNA-criteria GIN-28 p33 CL181019_022	DNA-criteria GCE-28 p16 CL181019_023	DNA-criteria GCE-28 p19 CL181019_024	DNA-criteria T28.3 CL181019_025
AM	X, X	X, X	X, X	X, Y	X, Y	X, Y	X, Y	X, Y
D3S1358	15, 16	15, 16	15, 16	14, 17	14, 17	14, 17	14, 17	14, 17
D1S1656	12, 16	12, 16	12, 16	12, 16	12, 16	12, 16	12, 16	12, 16
D6S1043	14, 18	14, 18	14, 18	11, 13	11, 13	11, 13	11, 13	11, 13
D13S317	12, 12	12, 12	11, 12	11, 12	11, 12	11, 12	11, 12	11, 12
Penta E	6, 9	6, 9	6, 9	7, 17	7, 17	7, 17	7, 17	7, 17
D16S539	12, 12	12, 12	12, 12	9, 12	9, 12	9, 12	9, 12	9, 12
D18S51	16, 17	16, 17	16, 17	14, 17	14, 17	14, 17	14, 17	14, 17
D2S1338	17, 19	17, 19	17, 19	19, 23	19, 23	19, 23	19, 23	19, 23
CSF1PO	11, 11	11, 11	11, 11	11, 13	11, 13	11, 13	11, 13	11, 13
Penta D	12, 13	12, 13	12, 13	12, 14	12, 14	12, 14	12, 14	12, 13, 14
TH01	9, 9	9, 9	7, 9	6, 9.3	6, 9.3	6, 9.3	6, 9.3	6, 9.3
vWA	17, ?	17, 17	17, 17	14, 15	14, 15	14, 15	14, 15	14, 15
D21S11	30, 30	30, 30	30, 30	27, 33	27, 33	27, 33	27, 33	27, 33
D7S820	9, 10	9, 10	9, 10	8, 10	8, 10	8, 10	8, 10	8, 10
D5S818	12, 13	12, 13	12, 13	11, 12	11, 12	11, 12	11, 12	11, 12
TPOX	8, 11	8, 11	8, 11	8, 11	8, 11	8, 11	8, 11	8, 11
D8S1179	10, 13	10, 13	10, 13	10, 14	10, 14	10, 14	10, 14	10, 14
D12S391	18, 18	18, 18	18, 18	20, 21	20, 21	20, 21	20, 21	20, 21
D19S433	13, 13	13, 13	13, 13	14, 14	14, 14	14, 14	14, 14	13, 14
FGA	21, 22	21, 22	21, 22	23, 25	23, 25	23, 25	23, 25	23, 25

Figure 3SI: Single tandem repeat genotyping of patient-derived GBM cell lines. Cell line authentication of the GIN-8, GIN-28, and GCE-28 patient-derived primary lines isolated from the GBM invasive edge. DNA was isolated from each sample and genetic characteristics determined by PCR-single-locus-technology, utilizing 21 independent PCR-systems. The GIN-8 line compared across two passages (p11 and p33), showed identical STR genotypes, which fully matched the STR genotype from primary invasive margin GBM tissue (T8.3) from which the cells were derived. The GIN-28 line compared across two passages (p11 and p33), showed identical STR genotypes, with 20/21 DNA systems matching the STR genotype from primary invasive margin GBM tissue (T28.3) from which the cells were derived. Similarly, the GCE-28 line compared across two passages (p16 and p19), showed identical STR genotypes, with 20/21 DNA systems matching the STR genotype from primary GBM tissue (T28.3) from which the cells were derived. Note that GIN-28 and GCE-28 are invasive margin and contrast enhanced cell lines derived from the same patient. Collectively these results confirm that the cell lines utilised in this study have not been cross-contaminated with any other cell line and the primary lines derived from the GBM invasive margin broadly retain the genotype of the tumour.

Metabolic Activity.

Cells were seeded at a density of 1×10^4 cells per well in 96 well plates (Corning) for 24 hours prior to assaying. Dosing of cells was initiated by removing culture medium, washing cells with phosphate buffered saline (PBS; Sigma-Aldrich) and the application of 100 μ L per well of treatment for 48 hours. Treatments were applied to cells in phenol red free DMEM (Thermo-Fisher) containing 10% BGS. Pyrazolo[3,4-*d*]pyrimidine-based kinase inhibitors were dosed at concentrations of 0.78 – 50.00 μ g/mL for determination of their half maximal inhibitor concentration (IC_{50}) values, and at 5 μ g/mL for evaluation of their activity in formulations. Additionally, to study the cytocompatibility of the DMSO concentration used to dissolve free drugs, medium containing 1% (v/v) DMSO was applied to cells. Cells were also treated with 0.1% (v/v) Triton-X 100 and DMEM with 10% BGS for 48 h for use as positive and negative controls, respectively. Following treatment, cells were washed with PBS and incubated with 100 μ l 10% PrestoBlue™ Cell Viability Reagent diluted in medium per well for 1 h. Solution fluorescence was then measured at 560/600 nm ($\lambda_{ex}/\lambda_{em}$), and relative metabolic activity calculated by setting the values of the negative control as 100% and the positive control (0.1% Triton X-100) as 0%. The metabolic viability graphs are reported in **Figure 4SI**.

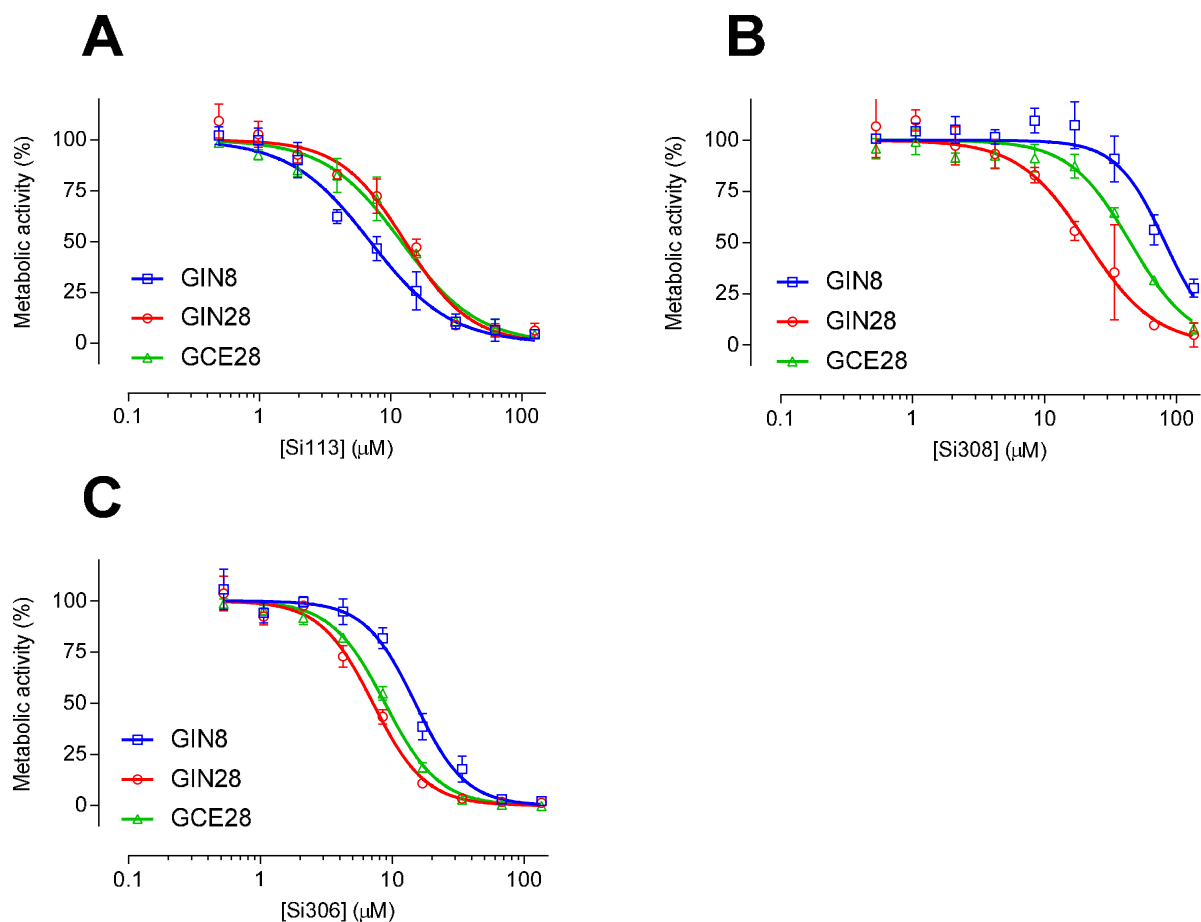


Figure 4SI. Effect of (A) SI113, (B) SI308 and (C) SI306 compounds on cellular metabolic activity as determined by the PrestoBlue assay. Compounds were applied diluted in 10% FBS containing DMEM for 48h. Data are presented as mean \pm SD (n=3).

In the **Figure 7** of the manuscript, compound SI306 formulated with the selected best polymers was tested against the patients derived GBM cell lines and the potency compared to the compound solubilized in 1% DMSO. The formulated compounds were diluted reaching a concentration of 5 $\mu\text{g}/\text{mL}$ and 45 $\mu\text{g}/\text{mL}$ for SI306 and the polymers, respectively (“drug”/polymer ratio of 10/90% w/w), using 10% FBS containing DMEM.

Detection of Activated Caspase-3/7.

The CellEvent caspase-3/7 green detection reagent (Thermo Fisher Scientific) was employed to evaluate levels of activated caspase-3 or -7. After exposure to the drugs solutions, 150 μL of 2% (v/v) CellEvent probe in PBS was applied per well for 30 min at 37 $^{\circ}\text{C}$. Staurosporine was used at 10 μM as the apoptotic control. Fluorescent intensity was measured at 502/530 nm ($\lambda_{\text{ex}}/\lambda_{\text{em}}$) and normalized to the untreated control (set as a value of 1).

Hoechst 33342/Propidium Iodide Microscopy.

Integrity of the nuclear membrane and nuclear fragmentation was measured by propidium iodide (PI; Thermo Fisher Scientific) uptake. To do so, 6×10^4 GIN28 and GCE28 cells per well were seeded in 24-well plates (Corning) and cultured for 24h. Following this, treatment solutions, including selected kinase inhibitors, or 100% ice cold ethanol were applied for 48h.

Treatments were then aspirated, and the cells were washed with PBS, followed by the addition of 1 μ M Hoechst 33342 (Thermo Fisher Scientific) in PBS for 5 min and then 0.1 mg/mL of PI in PBS (final concentration $\sim 2 \mu$ g/mL PI). The cells were incubated for another 5 min, after which the solution was removed, and the cells were washed with PBS. Cells were then imaged on an inverted Nikon Eclipse TE 300 microscope using a DAPI filter (357/447 nm; excitation/emission) for detection of the Hoechst signal and the RFP filter (531/593 nm; excitation/emission) for the PI signal.

Statistical analysis.

Dose-response curve fitting was performed using non-linear regression analysis to enable IC₅₀ determination (GraphPad prism, version 7.03). Statistical analysis was performed by one-way ANOVA with Dunnett's multiple comparison post hoc test using GraphPad prism.

Determination of Combination Index (CI) values

CI values were determined according to a widely used method established by Chou and Talalay.^{5,6} Briefly, in order to determine each CI value, the following cytotoxicity studies were conducted: (1) SI113 as a single compound, (2) SI308 as a single compound, (3) SI306 as a single compound, (4) S306 + SI308 combination, (5) SI113 + SI308 combination and (6) SI113 + SI306 combination. Compounds were applied in combination at a molar ratio of 1:1, and dosed with a range of 0.1 – 100.0 μ M per compound. IC₅₀ values were then calculated from each study and used in the following equation to determine CI values;

$$CI = \frac{D_{CA}}{D_{SA}} + \frac{D_{CB}}{D_{SB}} + \frac{D_{CA} D_{CB}}{D_{SA} D_{SB}}$$

Where D_{CA} represents the IC₅₀ values of drug A in combination with drug B, and D_{SA} the IC₅₀ of drug A as a single compound. Similarly, D_{CB} represents the IC₅₀ values of drug B in combination with drug A, and D_{SB} the IC₅₀ of drug B as a single compound. Based on this method, CI values are indicative of strong synergism (<0.7), synergism (0.7-0.9), additive effect (0.9-1.1), antagonism (1.1-3.3), or strong antagonism (>3.3).⁵ Microsoft Excel was then employed to produce a tricolor system based on these values, where antagonism is represented by red, additive effect by yellow, and synergism by green.

References

- (1) Tintori, C.; Fallacara, A. L.; Radi, M.; Zamperini, C.; Dreassi, E.; Crespan, E.; Maga, G.; Schenone, S.; Musumeci, F.; Brullo, C.; Richters, A.; Gasparrini, F.; Angelucci, A.; Festuccia,

C.; Delle Monache, S.; Rauh, D.; Botta, M. Combining X-ray crystallography and molecular modeling toward the optimization of pyrazolo[3,4-*d*]pyrimidines as potent c-Src inhibitors active in vivo against neuroblastoma. *J. Med. Chem.* **2015**, *58* (1), 347–361.

- (2) Tintori, C.; La Sala, G.; Vignaroli, G.; Botta, L.; Fallacara, A. L.; Falchi, F.; Radi, M.; Zamperini, C.; Dreassi, E.; Dello Iacono, L.; Orioli, D.; Biamonti, G.; Garbelli, M.; Lossani, A.; Gasparrini, F.; Tuccinardi, T.; Laurenzana, I.; Angelucci, A.; Maga, G.; Schenone, S.; Brullo, C.; Musumeci, F.; Desogus, A.; Crespan, E.; Botta, M. Studies on the ATP binding site of Fyn kinase for the identification of new inhibitors and their evaluation as potential agents against tauopathies and tumors. *J. Med. Chem.* **2015**, *58* (11), 4590–4609.
- (3) Radi, M.; Dreassi, E.; Brullo, C.; Crespan, E.; Tintori, C.; Bernardo, V.; Valoti, M.; Zamperini, C.; Daigl, H.; Musumeci, F.; Carraro, F.; Naldini, A.; Filippi, I.; Maga, G.; Schenone, S.; Botta, M. Design, Synthesis, biological activity, and ADME properties of pyrazolo[3,4-*d*]pyrimidines active in hypoxic human leukemia cells: a lead optimization study. *J. Med. Chem.* **2011**, *54* (8), 2610–2626.
- (4) Sanna, M.; Sicilia, G.; Alazzo, A.; Singh, N.; Musumeci, F.; Schenone, S.; Spriggs, K. A.; Burley, J. C.; Garnett, M. C.; Taresco, V.; Alexander, C. Water solubility enhancement of pyrazolo[3,4-*d*]pyrimidine derivatives via miniaturized polymer–drug microarrays. *ACS Med. Chem. Lett.* **2018**, *9* (3), 193–197. h
- (5) Chou, T.-C. Theoretical Basis, experimental design, and computerized simulation of synergism and antagonism in drug combination studies. *Pharmacol. Rev.* **2006**, *58* (3), 621–681.
- (6) Chou, T.-C. Drug Combination studies and their synergy quantification using the Chou-Talalay Method. *Cancer Res.* **2010**, *70* (2), 440–446.